

A New Approach for Fluid Flow Model in Gas Tungsten Arc Weld Pool Using Longitudinal Electromagnetic Control

The mathematical model of body force incorporates the additional magnetic field influence in the weld pool

BY J. LUO, Q. LUO, Y. H. LIN, AND J. XUE

ABSTRACT. In gas tungsten arc welding (GTAW), using a probe, the distribution of arc current density is measured with an additional longitudinal magnetic field. A model of the distribution of welding arc current flux is then modeled. Next, a new mathematical model of the body force is presented, which incorporates the additional influence of the magnetic field in the weld pool. Moreover, a model is developed for the fluid flow in the weld pool for the control process, which was based on experiments using LD10CS aluminum alloy. The boundary conditions are presented, and the influences of the additional longitudinal magnetic field and other factors are discussed using the equations describing the body forces.

Introduction

The arc welding technique that uses an additional electromagnetic field for control is called electromagnetic stirring. This technique is unlike standard arc welding techniques in that it offers the following advantages (Refs. 1–4):

- A low initial investment.
- An increase in operational reliability due to a high-performance coil.
- Higher mechanical quality from the fine crystal grain.
- A minimized risk of cold cracking because of the low hydrogen content.
- Exceptional appearance of the welding joints with clean weld surfaces.
- Increased environmental safety due to a lower magnetic field power.

This welding technique has a variety of applications in several fields, such as metallurgy, chemical engineering, manufacturing, electric power generation, aviation, and space flight (Refs. 2–8). Several aspects of welding with electromagnetic stirring have been analyzed previously.

J. LUO and J. XUE are with Xi'an JiaoTong University, China; Q. LUO is with Lian Yuan Steel & Iron Ltd. Company; and Y. H. LIN is with Shanghai Volkswagen Company.

These studies include research in solidification structure, cracking, arc behavior, metal transfer, weld formation, numerical simulation, mechanical ability, and quality improvement (Refs. 1–11). However, none of these studies have focused on the characterization of the fluid flow in the weld pool, which actually determines the effectiveness of using electromagnetic stirring.

When using longitudinal magnetic field control, the analysis of the body force is the key to understanding the fluid flow and heat transfer in the GTA weld pool. An analysis of the body force will assist in examining what effect an increase of the longitudinal magnetic field has on the GTA welding process. Therefore, the purpose of this paper is to define the body force and to model the fluid flow in the weld pool. In all the experiments, LD10CS aluminum alloy was used for simplicity and applicability.

Basic Theory

The application of the body force is not used in the standard GTAW process. The definition of the body force is the electromagnetic force applied to the fluid in the weld pool. It consists of the following two forces:

1) Self-electromagnetic force \vec{F}_{zm} generated by the interaction of the divergent current and its self-induced magnetic field in the weld pool.

2) Additional electromagnetic force \vec{F}_{wm} generated by the interaction of the divergent current and the additional longitudinal magnetic field in the weld pool.

Thus, the total electromagnetic force

\vec{F}_m in the incompressible molten metal fluid of the GTA weld pool can be expressed as:

$$\vec{F}_m = \vec{F}_{zm} + \vec{F}_{wm} \quad (1)$$

Adopting the fixed spot GTAW using longitudinal magnetic field control enables the calculation of the body force to be performed more simply. Starting with Maxwell's equation, the body force can begin to be described by the following equation:

$$\nabla \times \vec{B} = \mu_0 \vec{j} \quad (2)$$

Current Distribution

In direct current electrode negative (DCEN) GTAW undergoing additional longitudinal magnetic field control, a certain circumstance arises when using the nonmagnetic LD10CS aluminum alloy. The welding current flux density distribution on the surface of the weld pool is the same as the welding arc current flux density distribution on an interface between the welding arc and the weld pool. Thus, a probe method is used to measure the distribution of the welding arc current flux on this interface (Refs. 1, 4, 8). The experimental equipment used is shown in Fig. 1. The measurement values of the welding arc current flux distribution are shown in Fig. 2. These experiments were taken using a small welding current ($I = 100$ A) and weak magnetic field ($B < 0.1$ T).

The distribution character of the welding arc current flux can now be analyzed within these ranges of current and intensity of the magnetic field. A Gaussian distribution model of the welding arc current flux can be formulated using a numerical regression analysis as follows:

$$j(r)_{arc} = j_0 \square \frac{KI}{\pi} \exp[-K(r)^2] \quad (3)$$

KEY WORDS

GTAW
Body Force
Electromagnetic Stirring
Fluid Flow
Longitudinal Magnetic Field
Weld Pool

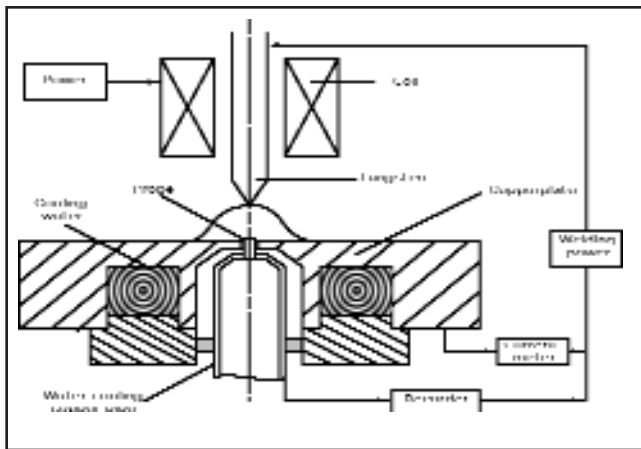


Fig. 1 — Diagram of measuring welding current flux distribution.

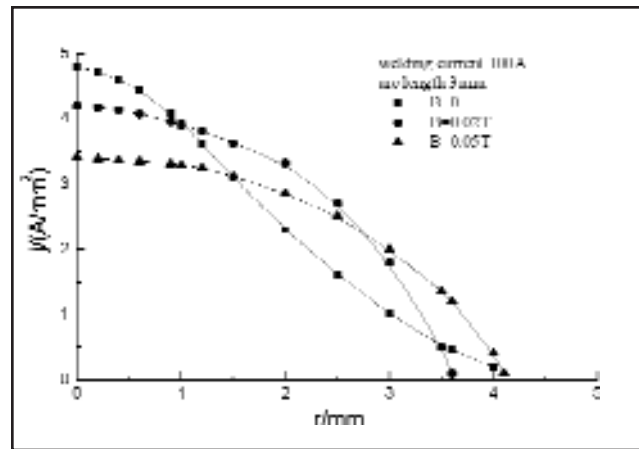


Fig. 2 — Measurement values and regression curves of welding current flux distribution.

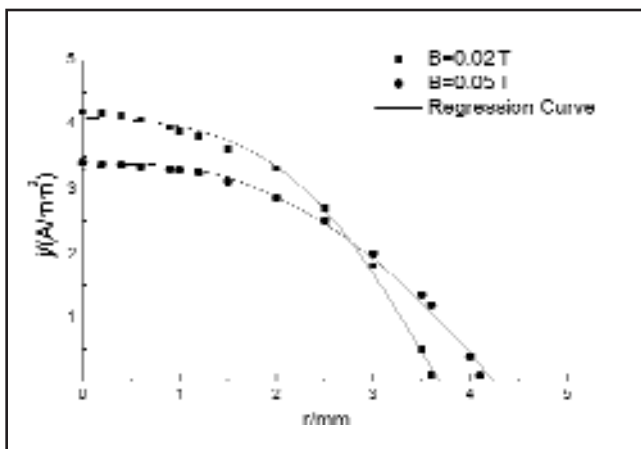


Fig. 3 — Regression curves of welding current flux distribution.

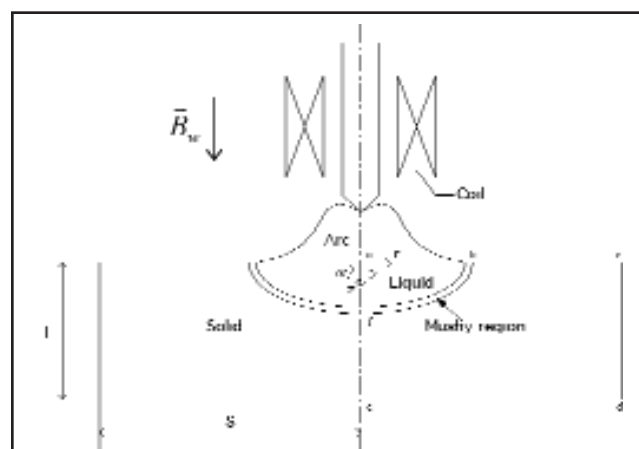


Fig. 4 — Schematic diagram of the weld pool and coordinates system.

where $j(r)_{arc}$ is the welding arc current flux distribution, a is the lumped coefficient (generally between 0.5~3; in this paper $a = 1$) and j_0 is the current flux density.

$$K = \frac{a}{2\sigma_j}$$

is the form of the gather coefficient of current flux.

When the welding current is 100 A, the magnetic induction was 0.02 T and 0.05 T. The regression curves of welding arc current flux distribution are shown in Fig. 3. As shown, the measured values fit the proposed model of the welding arc current flux distribution.

Body Force Equation

The cylindrical coordinate system (r, θ, z) (see Fig. 4) is selected in order to derive

the mathematical model of the body force in the GTA weld pool undergoing longitudinal magnetic field control. The vectors along the radial and axial directions, such as force, current flux, and magnetic induction, are expressed as two partial vectors (r, z) , respectively, and are symmetrical along the z -axis. Thus, the magnetic induction B can be expressed as

$$\vec{B} = [0, B_\theta(r, z), 0] \quad (4)$$

$$\nabla \times \vec{B} = \begin{bmatrix} \frac{1}{r} \frac{\partial}{\partial r} \left(\frac{f}{r} \right) \\ \frac{\partial}{\partial z} \left(\frac{f}{r} \right) \\ 0 \end{bmatrix}$$

$$= \begin{bmatrix} \frac{1}{r} \frac{\partial}{\partial r} \left(\frac{f}{r} \right) \\ \frac{\partial}{\partial z} \left(\frac{f}{r} \right) \\ 0 \end{bmatrix} B_\theta \quad (5)$$

The magnetic flow function is defined as

$$\psi_e = rB_\theta \quad (6)$$

Therefore, Equation 4 becomes

$$\nabla \times \vec{B} = \begin{bmatrix} -\frac{1}{r} \frac{\partial \psi_e}{\partial z} \\ 0 \\ \frac{1}{r} \frac{\partial \psi_e}{\partial r} \end{bmatrix} \quad (7)$$

Because, in Equation 2, the term $\mu_0 \vec{j}$ has the following form:

$$\mu_0 \vec{j} = \mu_0 (j_r, 0, j_z) \quad (8)$$

After substitution of Equations 7 and 8 into Equation 2, the corresponding part of the vector can be expressed as

$$\begin{bmatrix} j_r \\ j_z \end{bmatrix} = \begin{bmatrix} -\frac{1}{\mu_0} \frac{1}{r} \frac{\partial \psi_e}{\partial z} \\ \frac{1}{\mu_0} \frac{1}{r} \frac{\partial \psi_e}{\partial r} \end{bmatrix} \quad (9)$$

Moreover,

$$\vec{j} \langle \vec{B} = \begin{pmatrix} \downarrow \bar{r} & \bar{\theta} & \bar{z} \\ \in j_r & 0 & j_z \\ \in 0 & B_\theta & 0 \end{pmatrix} \quad (10)$$

$$\begin{aligned} (\vec{j} \langle \vec{B})_r &= -B_\theta j_z \\ (\vec{j} \langle \vec{B})_z &= B_\theta j_r \end{aligned} \quad (11)$$

According to Refs. 12–15, it is assumed that the electrical conductance is not temperature dependent. Thus,

$$\frac{f j_r}{f z} = 0 \quad (12)$$

Therefore,

$$\begin{aligned} \frac{f j_r}{f z} &= \frac{f}{f z} \left(-\frac{1}{\mu_0 r} \frac{f \Psi_e}{f z} \right) \\ &= -\frac{1}{\mu_0 r} \frac{f^2 \Psi_e}{f z^2} = 0 \end{aligned} \quad (13)$$

where Ψ_e satisfies

$$\Psi_e = C_1 z + C_2 \quad (14)$$

Note when $z = L$, then $\Psi_e = 0$ because there is not electronic magnetic flow at the bottom of the welding workpiece. When $z = 0$, then

$$\Psi_e = \frac{f \Psi_e}{f r} = \mu_0 j_z r$$

This is because the electronic magnetic flow on the surface of the welding workpiece (LD10CS aluminum alloy) is the same as the magnetic flow distribution of the welding arc on the interface between the welding arc and workpiece.

Thus, the magnetic flow function Ψ_e becomes

$$\Psi_e|_{z=0} = \int \mu_0 j_z|_{z=0} r dr \quad (15)$$

Moreover, according to Fig. 2, Equation 3, and Equation 15, assuming a small current ($I = 100$ A) and weak magnetic field ($B < 0.1$ T), the boundary condition can be described as follows:

$$j_z|_{z=0} = \frac{I}{2\pi\sigma_j} \exp\left(-\frac{r^2}{2\sigma_j^2}\right) \quad (16)$$

$$\begin{aligned} \Psi_e|_{z=0} &= \frac{I}{2\pi\sigma_j} \mu_0 \int_0^r \exp\left(-\frac{r^2}{2\sigma_j^2}\right) r dr \\ &= \frac{\mu_0 I}{2\pi} \left[\frac{1}{\sigma_j^2} - \exp\left(-\frac{r^2}{2\sigma_j^2}\right) \right] \quad (17) \end{aligned}$$

By solving the set of Equations 13, 14, and 17, the magnetic flow function Ψ_e can be given as

$$\Psi_e = \frac{\mu_0 I}{2\pi} \left[\frac{1}{\sigma_j^2} - \exp\left(-\frac{r^2}{2\sigma_j^2}\right) \right] \left(1 - \frac{z}{L} \right) \quad (18)$$

The current flux distribution of the GTA weld pool surface undergoing a longitudinal magnetic field is determined by the experimental measurement. Then the resulting (part something) is obtained from Fig. 2 and Equation 3.

Thus, Equation 6 can be expressed as

$$B_\theta = \frac{\Psi_e}{r} = \frac{\mu_0 I}{2\pi r} \left[\frac{1}{\sigma_j^2} - \exp\left(-\frac{r^2}{2\sigma_j^2}\right) \right] \left(1 - \frac{z}{L} \right) \quad (19)$$

After substituting Equation 18 into Equation 9, the current flux j of the LD10CS weld pool is given by

$$j = \frac{I}{2\pi\sigma_j^2} \exp\left(-\frac{r^2}{2\sigma_j^2}\right) \left(1 - \frac{z}{L} \right) \quad (20)$$

$$j_r = \frac{I}{2\pi L r} \left[\frac{1}{\sigma_j^2} - \exp\left(-\frac{r^2}{2\sigma_j^2}\right) \right] \quad (21)$$

After substituting Equation 19 into Equation 11, Equation 11 can be expressed as

$$\begin{aligned} (\vec{j} \langle \vec{B})_r &= -\frac{\mu_0 I^2}{4\pi^2 \sigma_j^2 r} \exp\left(-\frac{r^2}{2\sigma_j^2}\right) \\ &\left[\frac{1}{\sigma_j^2} - \exp\left(-\frac{r^2}{2\sigma_j^2}\right) \right] \left(1 - \frac{z}{L} \right) \end{aligned} \quad (22)$$

$$\begin{aligned} (\vec{j} \langle \vec{B})_z &= \\ &-\frac{\mu_0 I^2}{4\pi^2 L r^2} \left[\frac{1}{\sigma_j^2} - \exp\left(-\frac{r^2}{2\sigma_j^2}\right) \right] \left(1 - \frac{z}{L} \right) \end{aligned} \quad (23)$$

Then the self-electromagnetic force \vec{F}_{zm} in the weld pool is as follows:

$$\begin{aligned} \vec{F}_{zm} &= (\vec{j} \langle \vec{B})_r \\ &= -\frac{\mu_0 I^2}{4\pi^2 \sigma_j^2 r} \exp\left(-\frac{r^2}{2\sigma_j^2}\right) \\ &\left[\frac{1}{\sigma_j^2} - \exp\left(-\frac{r^2}{2\sigma_j^2}\right) \right] \left(1 - \frac{z}{L} \right) \end{aligned} \quad (24)$$

$$\begin{aligned} \vec{F}_{zmz} &= (\vec{j} \langle \vec{B})_z \\ &= \frac{\mu_0 I^2}{4\pi^2 L r^2} \left[\frac{1}{\sigma_j^2} - \exp\left(-\frac{r^2}{2\sigma_j^2}\right) \right] \left(1 - \frac{z}{L} \right) \end{aligned} \quad (25)$$

The additional electromagnetic force in \vec{F}_{wm} the weld pool is expressed as follows:

$$\vec{F}_{wm} = \vec{j}_r \langle \vec{B}_w \quad (26)$$

$$F_{wm} = \frac{I B_w}{2\pi L r} \left[\frac{1}{\sigma_j^2} - \exp\left(-\frac{r^2}{2\sigma_j^2}\right) \right] \quad (27)$$

where \vec{B}_w is the additional electromagnetic induction vector.

Therefore, the above formulations show that the electromagnetic force in the GTA weld pool undergoing a longitudinal magnetic field control (including the additional body force generated by the additional magnetic field) has polarity independence.

Model of Fluid Flow

Before introducing the mathematical model of fluid flow, certain definitions and assumptions need to be explained. There are three parts of the fluid velocity that are expressed as the radial velocity (v), axial velocity (u), and circumferential velocity (ω) in the directions of r , z , and θ , respectively (see Fig. 4). Moreover, there is an energy exchange, mass transfer, and heat transfer between the welding arc and the weld pool. Where the arc heat flux density $q(r)$ and the current flux density σ_j are distributed on the surface of the welding workpiece, $z = 0$. Lastly, the following conditions are assumed:

1) The surface of the weld pool is like a constant plane and the molten liquid metal in the weld pool is a Newton Body, which is a safe assumption when the arc welding current is less than 200 A.

2) The welding current is $I < 200$ A and the magnetic field is $B < 0.1$ T, where the distribution and current flux have a Gaussian distribution.

As shown in Fig. 4, let $u = u(r, z)$, $v = v(r, z)$, and $\omega = \omega(r, z)$ denote the velocity components in the axial z and radial r directions, respectively. The model of fluid flow would then be given as

$$\frac{1}{r} \frac{f(rv)}{fr} + \frac{f(u)}{fz} = 0 \quad (28)$$

$$\rho \left[\frac{fv}{ft} + v \frac{fv}{fr} + u \frac{fv}{fz} - \frac{\omega^2}{r} \right]$$

$$= F_r - \frac{fP}{fr} + \mu \left[\frac{f^2v}{fr^2} + \frac{1}{r} \frac{fv}{fr} - \frac{v}{r^2} + \frac{f^2v}{fz^2} \right]$$

$$\rho \left[\frac{fu}{ft} + v \frac{fu}{fr} + u \frac{fu}{fz} \right]$$

$$= F_z - \frac{fP}{fz} + \mu \left[\frac{f^2u}{fr^2} + \frac{1}{r} \frac{fu}{fr} + \frac{f^2u}{fz^2} \right] \quad (29)$$

$$\rho C_p \left[\frac{fT}{ft} + v \frac{fT}{fr} + u \frac{fT}{fz} \right]$$

$$= \frac{1}{r} \frac{f}{fr} k_r \frac{fT}{fr} + \frac{f}{fz} k_z \frac{fT}{fr} \quad (30)$$

The fluid flow in the weld pool is governed by a combination of factors. In view of Equation 29 with regard to Equations 24, 25, and 27, the body force, electromagnetic force, and buoyant force can each be expressed as the following:

$$F_z = -\frac{\mu_m I^2}{4\pi^2 L r^2} \left[1 - \exp\left(-\frac{r^2}{2\sigma_j^2}\right) \right]$$

$$\left\langle \left(1 - \frac{z}{L}\right) - \rho g \beta (T - T_i) \right\rangle \quad (31)$$

$$F_r = -\frac{\mu_m I^2}{4\pi^2 \sigma_j^2 r} \exp\left(-\frac{r^2}{2\sigma_j^2}\right)$$

$$\left\langle \frac{1}{r} \left[1 - \exp\left(-\frac{r^2}{2\sigma_j^2}\right) \right] \left(1 - \frac{z}{L}\right)^2 \right\rangle \quad (32)$$

$$F_\theta = \frac{IB_w}{2\pi L r} \left[1 - \exp\left(-\frac{r^2}{2\sigma_j^2}\right) \right] \quad (33)$$

Boundary Condition

For this model, the boundary conditions are ascertained from Equations 28–30 and are shown in Table 1.

Q_{arc} and Q_{loss} are defined as the heat input and heat loss, respectively. These terms are described as follows:

$$Q_{loss} = h_c(T - T_0) + Se(T^4 - T_0^4) \quad (34)$$

$$Q_{arc} = \frac{Q}{2\pi\sigma_q^2} \exp\left(-\frac{r^2}{2\sigma_q^2}\right) \text{ at } z = 0 \quad (35)$$

$$Q = \eta I U \quad (36)$$

$$T = T_m, \text{ at the liquid-solid boundary.} \quad (37)$$

Conclusion

The welding properties for GTAW undergoing a longitudinal magnetic field

Table 1 – Boundary Condition

Side	U	V	ω	T
Ab	0	0	0	$-k \frac{fT}{fz} = Q_{arc} - Q_{loss}$
Bc	0	0	0	$-k \frac{fT}{fz} = Q_{loss}$
Cd	0	0	0	$T = T_x$
De	0	0	0	$-k \frac{fT}{fz} = Q_{loss}$
Ef	0	0	0	$\frac{fT}{fr} = 0$
Fa	$\frac{fu}{fr} = 0$	0	0	$\frac{fT}{fr} = 0$

control are different from the standard GTAW. The critical differences found from the research are summarized as follows:

1) The electromagnetic body forces in the weld pool include the self-electromagnetic force and the additional electromagnetic force. Also, the electromagnetic forces are independent of welding polarity. Moreover, by using a probe method, the current flux distribution on the surface of the LD10CS weld pool can be detected by measuring the arc current flux distribution. Then the welding arc current density distribution can be modeled. Finally, then the mathematical model of the body force in the LD10CS GTA weld pool undergoing a longitudinal magnetic field control is defined.

2) In addition, a new model of fluid flow in the weld pool was developed. This was done by examining the dynamics between the additional longitudinal magnetic field and the self-electromagnetic field, which accounts for the other body forces and the heat transferred. The boundary conditions were also provided. Thus, the model sufficiently described the electromagnetic field, the velocity field, and the thermal field on process. The model is, therefore, a comprehensive description for the fluid flow on GTA weld pool undergoing a longitudinal magnetic field.

Acknowledgments

The authors acknowledge Associate Prof. Y. M. Zhang of the University of Kentucky, Prof. C. S. Jia of Xi'an JiaoTong University, Prof. C. S. Wu of ShangDong University of Technology, Prof. Y. X. Wu

of Shanghai JiaoTong University, National Natural Science Foundation of China (NSFC), and China Postdoctoral Science Foundation (CPSF). The projects are supported by the NSFC (serial: 59775059) and CPSF.

List of Symbols

- ρ density (kg·m³)
- P pressure (Pa)
- I welding current (A)
- j current flux density (A·m²)
- B the magnetic induction (T)
- B_w additional magnetic induction (T)
- σ_j distribution parameter of current density (A·m²)
- L thickness of welding workpiece (m)
- β coefficient of thermal expansion (K⁻¹)
- g acceleration of gravity (m·s⁻²)
- T temperature (K)
- t time (s)
- C_p specific heat of workpiece (J·kg⁻¹·K⁻¹)
- T_l melting point of workpiece (K)
- μ dynamic viscosity (kg·m⁻¹·s)
- k thermal conductivity of molten metal (W·m⁻¹·K⁻¹)
- δ thickness of workpiece (m)
- μ_0 magnetic permeability (H·m⁻¹), $\mu_0 = 4\pi \times 10^{-7}$ H/m
- T_0 initial temperature (K)
- h_c convection heat transfer coefficient (W·m⁻²·K⁻¹)
- S Stefan-Boltzmann coefficient (W·m⁻²·K⁻⁴)
- q_{loss} heat loss per unit time (W·m⁻²)
- q_{arc} heat input per unit time (W·m⁻²)

References

1. Jia, C. S., Yin, X. Q., and Jia, T. 1994. The welding arc behavior in longitudinal magnetic

field. *Journal of Xi'an JiaoTong University* 28(4): 7-13.

2. Matsuda, F., Nakagawa, H., and Nakata, K. 1978. Effect of electromagnetic stirring on weld solidification structure of aluminum alloys, Report I — Investigation on GTA weld metal of thin sheet. *Trans. of JWRI* 7(1): 111-126.

3. Matsuda, F., Nakata, K., and Miyanaga, Y. 1978. Effect of electromagnetic stirring on weld solidification structure of aluminum alloys, Report II — Investigation on GTA in DCSP weld metal of 8 mm thick plate. *Trans. of JWRI* 7(2): 33-45.

4. Yin, X. Q., Li, H. G., and Luo, J. 1998. Study on the elimination of weld hot-cracking of LD10CS aluminum alloy with electromagnetic stirring. *Journal of Xi'an JiaoTong University* 32(5): 91-96.

5. Luo, J., Jia, T., Yin, X. Q., Xue, J., and Jia, C. S. 1999. Numerical calculation and influence of the external intermittent and alternative longitudinal magnetic field in stainless steel GTA welding. *ACTA Metallurgical Sinica* 35(3): 330-334.

6. Kuznetsov, V. D. 1972. Behaviors of the arc and transfer of electrode metal on welding

process in a longitudinal magnetic field. *Welding Production* 19(4): 1-4.

7. Selyanenkov, V. N. 1975. Formation of the weld pool in a longitudinal magnetic field in argon-arc welding. *Welding Production* 22(1): 50-53.

8. Li, H. G., Yin, X. Q., Luo, J., Jia, C. S., and Sun, B. 1998. Improving weld quality of LD10CS aluminum alloy by electromagnetic stirring. *Transactions of the China Welding Society* 19 (supplement): 100-105.

9. Yu, J. R., Zhang, J. Y., and Jia, C. S. 1997. Contracted effect of bell-shade shape welding arc and accompanied magnetic field with spiral pipe shape. *Transactions of Nonferrous Metals Society of China* 7(2): 95-98.

10. Jia, C. S., Luo, J., and Jia, T. 1999. Investigation on the control of porosities in GTA weld with longitudinal intermittent alternative magnetic fields. *Aeronautical Manufacturing Technology* 198(3): 26-29.

11. Luo, J., Jia, C. S., and Wang, Y. S. 2001. Effect of longitudinal intermittent alternative magnetic field on weld formation in tungsten inert-gas arc welding. *Aeronautical Manufacturing Technology* 217(4): 38-42.

12. Oreper, G. M., and Szekely, J. 1984.

Heating and fluid-flow phenomena in weld pools. *J. Fluid Mech.* 147(2): 53-59.

13. Mills, G. S. 1980. Arc physics and weld pool behavior. *Welding Journal* 59(1): 11-s to 18-s.

14. Ushio, M., and Wu, C. S. 1997. Mathematical modeling of three-dimensional heat and fluid flow in a moving gas metal arc weld pool. *Metall. Trans.* 28B(6): 509-16.

15. Choo, R. T. C., David, S. A., and Vitek, J. M. 1991. Effect of evaporation and temperature-dependent material properties on weld pool development. *Welding Journal* 70(9): 223-s to 233-s.

16. Zacharia, T., David, S. A., and Vitek, J. M. 1991. Computational modeling of stationary gas-tungsten weld pools and comparison to stainless steel 304 experimental results. *Metall. Trans.* 22B(4): 243-57.

17. Tasi, M. C., and Kou, S. 1990. Electromagnetic-force-induced convection in weld pools with a free surface. *Welding Journal* 69(6): 241-s to 246-s.

18. Kou, S., and Wang, Y. H. 1986. Computer simulation of convection in moving and arc weld pools. *Metall. Trans.* 17A (12): 2271-77.

Preparation of Manuscripts for Submission to the *Welding Journal* Research Supplement

All authors should address themselves to the following questions when writing papers for submission to the Welding Research Supplement:

- ◆ Why was the work done?
- ◆ What was done?
- ◆ What was found?
- ◆ What is the significance of your results?
- ◆ What are your most important conclusions?

With those questions in mind, most authors can logically organize their material along the following lines, using suitable headings and subheadings to divide the paper.

1) **Abstract.** A concise summary of the major elements of the presentation, not exceeding 200 words, to help the reader decide if the information is for him or her.

2) **Introduction.** A short statement giving relevant background, purpose, and scope to help orient the reader. Do not duplicate the abstract.

3) **Experimental Procedure, Materials, Equipment.**

4) **Results, Discussion.** The facts or data obtained and their evaluation.

5) **Conclusion.** An evaluation and interpretation of your results. Most often, this is what the readers remember.

6) **Acknowledgment, References and Appendix.**

Keep in mind that proper use of terms, abbreviations, and symbols are important considerations in processing a manuscript for publication. For welding terminology, the *Welding Journal* adheres to AWS A3.0:2001, *Standard Welding Terms and Definitions*.

Papers submitted for consideration in the Welding Research Supplement are required to undergo Peer Review before acceptance for publication. Submit an original and one copy (double-spaced, with 1-in. margins on 8 1/2 x 11-in. or A4 paper) of the manuscript. Submit the abstract only on a computer disk. The preferred format is from any Macintosh® word processor on a 3.5-in. double- or high-density disk. Other acceptable formats include ASCII text, Windows™, or DOS. A manuscript submission form should accompany the manuscript.

Tables and figures should be separate from the manuscript copy and only high-quality figures will be published. Figures should be original line art or glossy photos. Special instructions are required if figures are submitted by electronic means. To receive complete instructions and the manuscript submission form, please contact the Peer Review Coordinator, Doreen Kubish, at (305) 443-9353, ext. 275; FAX 305-443-7404; or write to the American Welding Society, 550 NW LeJeune Rd., Miami, FL 33126.